Design and Control of a flexibleOnboard Charger for Electric Vehicles with FOPI-Controlled Power Converters

JANAPATI SRAVANTHI [1] | S.NAGANNA[2]

[1]Pg Scholar, Dept of EPS, Kodada Institute of Technology & Science for Women-Kodad, Telangana.

[2] Assistant Professor, Dept of EEE, Kodada Institute of Technology & Science for Women-Kodad,Telangana.

ABSTRACT: Accurate operation of different power converters is crucial to the functioning of grid-integrated solar photovoltaic (PV) systems used by electric vehicles (EVs). The present work introduces a unique flexible board charge (OBC) for electric vehicles that may serve several purposes, all while controlling the power converter using fractionally ordered PI controllers (FOPI). The grid-integrated PV module was supplemented with energy storage components, including high-voltage and low-voltage batteries, to improve the OBC's overall performance dependability. To lessen the impact of semiconductor switching and switching losses, a model of an active voltage decoupling (APD) circuitry is used. This has the potential to improve efficiency while reducing the necessary DC-link capacitance. This study created a FOPI controller for use in controlling and operating power converters. The capacity to charge both HVB & LVB batteries concurrently is a notable feature of the proposed OBC, which allows it to generate substantial power via the solar roof. The DC connection voltage is maintained at a constant value, free of ripples, using the suggested FOPI controller. The goal of this simulation research was to evaluate the OBC's performance in four different ideal modes: grid-to-vehicle, the grid-to-, H2L, and HP2L, which stands for high-voltage bank to low-voltage battery. The suggested FOPI-based power converters in order for EV OBC applications deliver respectable output values across all modes.

KEYWORDS: OBC, FOPI, PV, EV, DC-LINK.

I.INTRODUCTION:

A CLASSIFICATION of ELECTRIC VEHICLES (EVs) is based on whether they are fully electric or hybrid. Electric vehicles' rising appeal on a worldwide scale is a result of the fact that they provide a viable transportation option for reducing carbon emissions. With the help of government incentives and large expenditures, the number of electric cars (EVs) on the road jumped thrice in only three years, reaching 16.5 million in 2021 (when only light-duty passenger vehicles were included) [1]. A dependable, efficient, and high-power-density-capable power converter is an essential part of any electric vehicle [2]. A common method for charging high-voltage battery (HVBs, 400 V) is using an integrated charger (OBC) that draws power from the electrical grid. In order to power a traction motor, the HVB's electric energy is transformed into kinetic energy using an inverter. A low voltage dc-dc converter (LDC), which is usually provided by the HVB, charges low-voltage batteries (12 V). Headlights, the control board, the music system, and the navigation system are all powered by the LVB. A lot of recent work has been on finding ways to combine the two types of power converters—OBC and LDC—into one integrated or multifunctional OBC [3, 4, 5, 6, 7, 8, 9, 10]. In addition, the total amount and cost of hardware may be decreased by sharing some of the electrical conversion components. Two primary methods may be used to classify this kind of study. Since passive components take up the most room in the OBC, reducing their size is the first point. Adding an active power decoupling (APD) circuitry may decrease the dc-link capacitance [11], enabling the use of longer-life film capacitors instead of aluminium electrolytic capacitors. An APD circuit that may absorb ripple energy from a single-phase circuit or charge the LVB from the HVB via relay operation was suggested by Nguyen et al. [3].

Realising a mode where the HVB or LVB may be charged at the same time is the second strategy [4, 5, 6]. Typically, the LDC will charge the LVB using the HVB. Charging both the LVB and the HVB at the same time from the AC grid is possible with an integrated OBC. A separate transformer [6] or a combination of winding transformer [4, 12] may both be used to achieve simultaneous charging. Nonetheless, prior research on concurrent charging has shown that the power required to charge the LBV should reduce the available HVB capacity. As an example, in simultaneous charging mode, the 3.3-kW converter designed by Kim et al. [6] only charged the LVB with 0.3 kW with the HVB with 3.0 kW. A revision of the OBC's power components is necessary to raise the LVB's capability. In solitary mode, the LDC may be run at full power; however, while charging many devices at once, its power is decreased. Electric vehicle (EV) solar roof technology has been the subject of many research projects. Mounting a solar roof on top of an electric vehicle isn't without its challenges, however, including inconsistent sunshine and efficiency limitations. The impact of sun rays on the electricity production of a solar roof installed on a Prius made by Toyota was the primary focus of Schuss et al. To address the issues related to partial shade of the solar roof, a differential energy processing converter was suggested. For optimal charging efficiency, Hyundai integrates the solar roof directly with the battery system via the converter. However, Toyota's system involves an additional solar battery that must be charged before the electricity from the solar roof can be used, which might potentially lower the charging efficiency. Both approaches, however, rely on individual power an converter, which reduces power density and makes it more difficult to systematically integrate, regulate, and communicate with all modes. Some have suggested noninsulated OBCs as a space-saving hardware option that satisfies the requirements of the SAE J1772 regulation [7, [8], [9], [10]. On the other hand, electric shocks and other safety issues might arise from a significant common-mode current when galvanic isolation is not present.

II. PROPOSED SYSTEM LAYOUT:

Fig. 1 illustrates the schematic structure of the proposed OBC for EVs. The circuit topology mainly composed with various components that are two energy sources such as grid and solar, two batteries (LVB & HVB), active switches, diodes, and a relay.

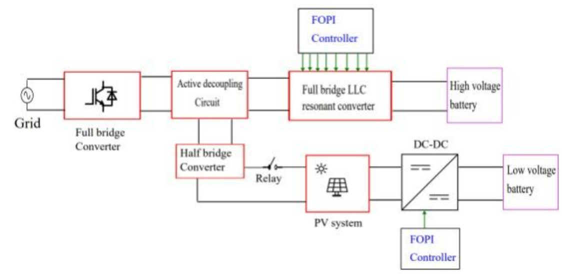

Fig.1 Structure of the proposed multipurposed OBC for the EV

This proposed OBC topology is incorporated with multiple power conversion stages:

- AC-DC Stage:
  - ➢ Employs a split-cap active power decoupling (APD) circuit to reduce capacitor size.
  - ➢ Shares a full-bridge (FB) converter with the DC-DC stage.
  - ➢ Integrates a high-frequency (HF) transformer for both decoupling and LVB charging.
- DC-DC Stage:
  - ➢ Work as an LLC resonant circuit for HVB charging in forward mode.

- Functions as a DABcircuit for HVB discharging (V2G).
- Shares the FB converter with the AC-DC stage.
- LVB Charging:
- Utilizes an isolated FB converter with diodes for LVB voltage regulation.
- Solar Integration:
- Incorporates a buck converter with an active switch (S_{13}) to enable MPPT operation from the solar roof.
- Allows for selective disconnection of the PV system from the LVB charging path.

III Proposed FOPI controller:

FOPI controllers offer a promising approach to improving the performance of power converters over traditional PI control. By leveraging the unique properties of fractional calculus, these controllers can achieve superior transient response, robustness, and tracking accuracy. This algorithm include manage the flow of power between the various components of the system, including the Solar-PV, grid, and EV chargers.

The Design of a customized FOPI control algorithm specifically tailored for the dynamics of the EV charger system is presented in this section. Another benefit of this proposed FOPI based EV charger is the nature of the current flowing through the motor's leakage inductance. Unlike some other charger designs, this system ensures the current is a clean sinusoid at the grid frequency.

FOPI control law mathematically defined as

$$C(s) = Kp + \frac{Ki}{s^{\lambda}}$$

λ value numerically varies from [0 to unity]. In other hand, in terms of frequency bounds (ω_b, ω_h) FOPI controller expressed as:

$$K(s) = \llbracket(1 + bs/d\omega b)/(1 + bs/d\omega h)\rrbracket$$
$$\hat{}\lambda$$

Where s=jw, b>0, d>0, and

In frequency bounds of $\omega b < \omega < \omega h$ Taylor polynomial expansion form as:

$$K(s) = \llbracket \frac{bs}{d\omega b}]\hat{}\lambda(1 + \lambda P(S) +$$
$$\frac{\lambda(\lambda-1)}{2}p\hat{}2(s)$$

Where $p(s) = \frac{-ds^2+d}{ds^2+b\omega hs}$

It is initiated that

$$s^{\lambda} = \frac{(d\omega b)^{\lambda b-\lambda}}{\left[1+\lambda P(S)+\frac{\lambda(\lambda-1)}{2}p^{2(s)}\right]}\left(\frac{1+\frac{bs}{d\omega b}}{1+\frac{ds}{d\omega h}}\right)^{\lambda}$$

Approximated the taylor polynomial implies to

$$S^{\lambda} = \frac{d\omega b}{b}\frac{ds^2+b\omega hs}{d(1-\lambda)s^2+b\omega hs+d\lambda}\left(\frac{1+\frac{bs}{d\omega b}}{1+\frac{ds}{d\omega h}}\right)^{\lambda}$$

The FO is given as

$$S^{\lambda} = \frac{d\omega b}{b}\frac{ds^2+b\omega hs}{d(1-\lambda)s^2+b\omega hs+d\lambda}\left(\frac{1+\frac{bs}{d\omega b}}{1+\frac{ds}{d\omega h}}\right)^{\lambda}$$

The genuine part's negative poles are in the range of [0 to 1]. Continuous-time coherent simulation is used to approximate equation:

$$K(s) = \lim_{n\to\infty} Kn(s) = \lim_{n\to\infty} = -N\frac{1+\frac{s}{\dot{\omega}k}}{1+\frac{s}{\omega k}}$$

The MATLAB layout of FOPI control scheme for FB and DC-DC converter are configured in fig.2 and fig.3 respectively.

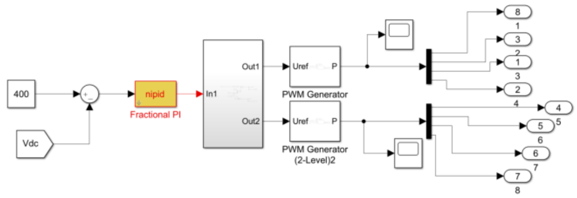

Fig.2. FOPI control scheme for operate the FB converter

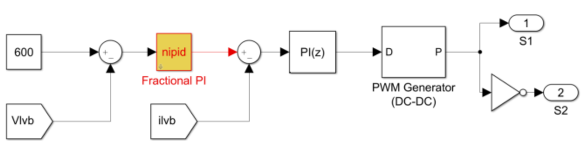

Fig.3. FOPI control scheme for operate the DC-DC converter

IV Simulation results:

To examine the effectiveness of proposed FOPI controller the OBC verified for various case studies as follows:

Mode 1 (G2V):

In this case study, the HVB is charged directly from the AC grid. The tertiary stage is deactivated by switching off the active switch, preventing power flow to the LVB. The APD circuit operates in buck or boost mode, utilizing the magnetizing inductance of the high-frequency transformer (TR2) to mitigate voltage ripple on the DC link.

The simulation results of grid voltage and grid current at unity PF in this mode is configured in fig.4a and fig.4b respectively.

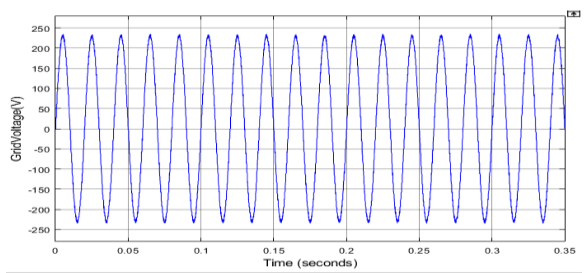

Fig.4a Grid voltage

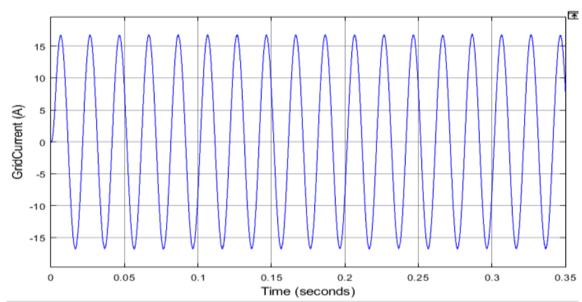

Fig.4b Grid current

To attain the rated DC link voltage (see fig.4d)of 400 V (Vdc_1+Vdc_2) the output voltages of FB converter regulated at 200V. The output voltage of FB converter (Vdc_1) is shown in fig.4c

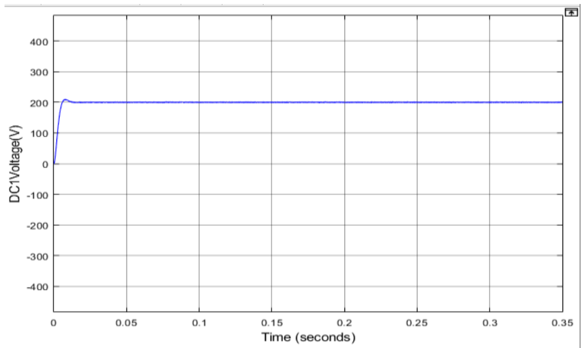

Fig.4cDC link voltage (V_{dc1})

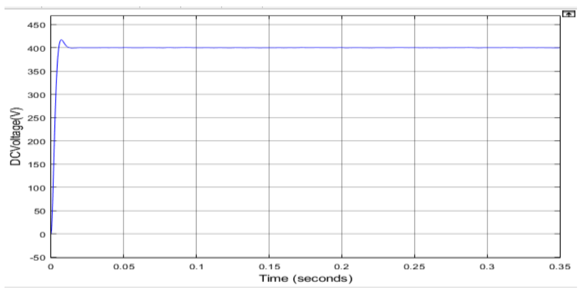

Fig.4d common DC link voltage

The simulation response of %SOC of battery (20Vconstant voltage) and inductor currents (ripple free) in this mode is shown in fig.4e and fig.4f respectively.

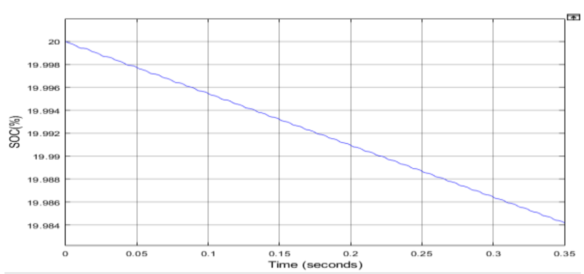

Fig.4e % SOC of battery

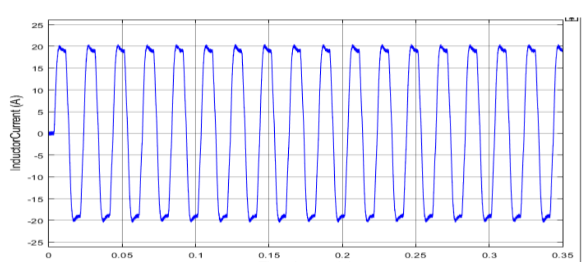

Fig.4f inductor current

Mode 2 (V2G):

This V2G operation is happened when vehicle as parked or during night hours. The HVB supplies power back to the grid. Similar to Mode 1, the tertiary stage is deactivated by opening switch S_{13} and the relay. The system utilizes the same topology as a conventional DC-AC inverter to control grid current and maintain DC link voltage. However, due to the inherent asymmetry of the LLC resonant converter, limitations arise in reverse power flow operation. Specifically, only buck operation is feasible, and the operating points significantly differ from those observed in forward power flow. If the SoC of the HVB is insufficient, its voltage may drop, potentially compromising the DC link voltage and hindering the ability of the DC-AC inverter to maintain grid synchronization.

Mode 3 (H2L):

This mode is associated to case study of the HVB-to LVB charging. Sufficient amount LVB charging is required to supports the mode 2 such as V2G operation. This mode doesn't require PV. To charge the LVB to its peak value of %SoC relay would be closed.This approach mainly related to drive the vehicle in light load condition. The simulation responses of primary and secondary voltages of HF transformer is represents in fig.5a and fig.5b

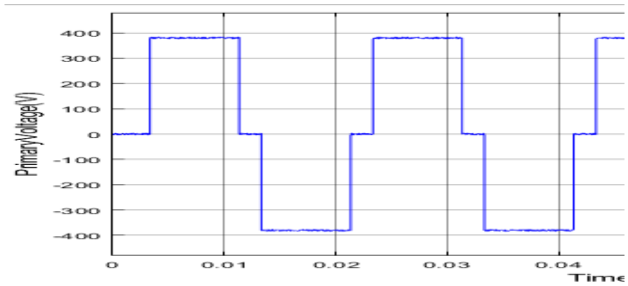

Fig.5a primary voltage

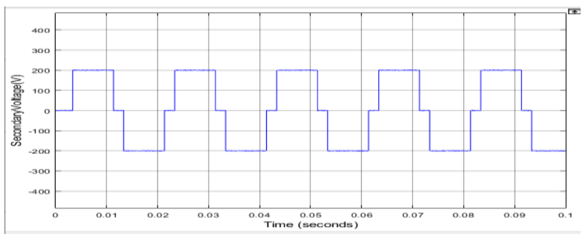

Fig.5b Secondary voltage

To regulate the common DC link voltage at 400V (see Fig.5d), the HBV charges the LVB up to its maximum value that is 12V. Fig, 5c shows the simulation response of voltage of LVB.

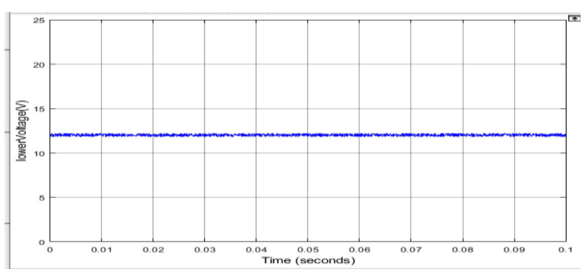

Fig.5c Lower voltage

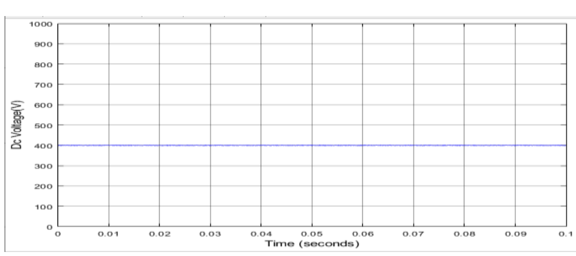

Fig.5d Common DC link voltage

Mode 4 (H2L):

The operation this mode is charge the LVB with both HVB and PV. For this operation solar network connected to the circuit topology. PV voltage (see fig.6b) generation highly depends on the availability of the solar irradiance levels. The available solar irradiance levels in this work is configure in fig.6a. To extract more PV power utilized INC MPPT approach.

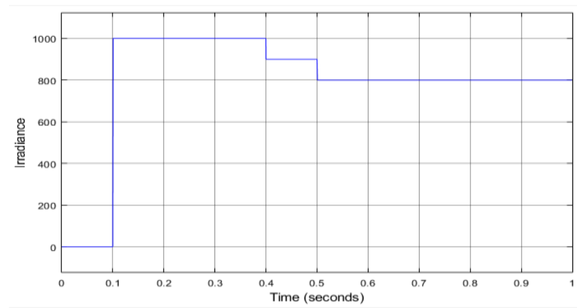

Fig.6a Solar irradiance levels

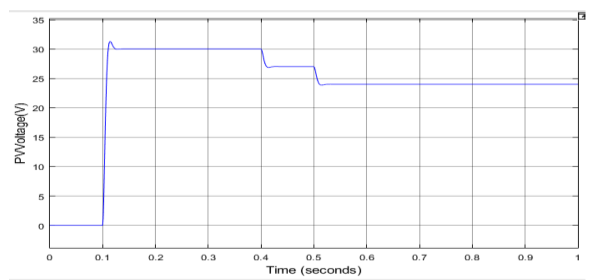

Fig.6a PV voltage

V Conclusions:

This study introduced a new kind of multi-function on-board charger (OBC) for electric vehicles (EVs) that use solar photovoltaic (PV) modules built into HVB and LVB battery. The proposed OBC has power conversion stages that can handle several operating modes, such as G2V (grid-to-hydro-power) and V2G (grid-to-hydro-disposal), H2L (hydro-to-load) and HVB-to-photovoltaic (PV) charging of the LVB. It is clear from the simulation results that the DC link voltage remained consistent across all of these operating modes. The integration of an APD circuit within the OBC improves efficiency and power density. Using an APD circuit reduces the amount of dc-link capacitance that is needed. The suggested FOPI controller effectively controls the power converters in different operating modes. One benefit of this suggested OBC is that it may charge the HVB both LVB batteries at the same time, making efficient use of the electricity from the solar-PV module.

REFERENCES:

[1] International Energy Agency. (Jun. 2022). Global EV Outlook 2022. IEA, France, Paris. [Online]. Available: https://www.iea.org/

[2] B. Bilgin et al., “Making the case for electrified transportation,” IEEE Trans. Transport. Electrific., vol. 1, no. 1, pp. 4–17, Jun. 2015.

[3] S. Kim and F.-S. Kang, “Multifunctional onboard battery charger for plug-in electric vehicles,” IEEE Trans. Ind. Electron., vol. 62, no. 6, pp. 3460–3472, Jun. 2015.

[4] Y.-S. Kim, C.-Y. Oh, W.-Y. Sung, and B. K. Lee, “Topology and control scheme of OBC–LDC integrated power unit for electric vehicles,” IEEE Trans. Power Electron., vol. 32, no. 3, pp. 1731–1743, Mar. 2017.

[5] PV-Powered Vehicle Strategy Committee Interim Report, New Energy and Industrial Technology Development Organization, Kanagawa, Japan, 2018.

[6] Trends in Photovoltaic Applications 2019, International Energy Agency Photovoltaic Power Systems Programme, Rheine, Germany, 2019.

[7] C. Schuss, T. Fabritius, B. Eichberger, and T. Rahkonen, “Impacts on the output power of photovoltaics on top of electric and hybrid electric vehicles,” IEEE Trans. Instrum. Meas., vol. 69, no. 5, pp. 2449–2458, May 2020.

[8] M. Uno, H. Sato, and T. Ishikawa, “Differential power processing converter enhancing energy yield of curved solar roofs of plug-in hybrid electric vehicles,” IEEE Trans. Veh. Technol., vol. 69, no. 12, pp. 14689–14700, Dec. 2020.

[9] R. Hou and A. Emadi, “Applied integrated active filter auxiliary power module for electrified vehicles with single-phase onboard chargers,” IEEE Trans. Power Electron., vol. 32, no. 3, pp. 1860–1871, Mar. 2017.

[10] J. G. Pinto, V. Monteiro, H. Gonçalves, and J. L. Afonso, “Onboard reconfigurable battery charger for electric vehicles with tractionto-auxiliary mode,” IEEE Trans. Veh. Technol., vol. 63, no. 3, pp. 1104–1116, Mar. 2014.